ESC European Society of Cardiology

European Heart Journal (2021) **42**, 3786–3799
doi:10.1093/eurheartj/ehab503

TRANSLATIONAL RESEARCH
Heart failure and cardiomyopathies

3′ untranslated region of *Ckip-1* inhibits cardiac hypertrophy independently of its cognate protein

Yinlong Zhao[1,2], Shukuan Ling[1]*, Jianwei Li[1], Guohui Zhong[1], Ruikai Du[1], Youyou Li[1], Yanqing Wang[1], Caizhi Liu[1], Xiaoyan Jin[1], Wei Liu[3], Tong Liu[3], Yuheng Li[1], Dingsheng Zhao[1], Weijia Sun[1], Zizhong Liu[1], Zifan Liu[1,4], Junjie Pan[1,5], Xinxin Yuan[1], Xingcheng Gao[1], Wenjuan Xing[1], Yan-Zhong Chang[2]*, and Yingxian Li[1]*

[1]State Key Laboratory of Space Medicine Fundamentals and Application, China Astronaut Research and Training Center, No.26 Beiqing Road, Haidian District, Beijing 100094, China; [2]Laboratory of Molecular Iron Metabolism, Key Laboratory of Molecular and Cellular Biology of Ministry of Education, College of Life Science, Hebei Normal University, No.20 Road East 2nd Ring South, Yuhua District, Shijiazhuang 050200, China; [3]Department of Cardiology, Beijing AnZhen Hospital, Capital Medical University, No.2 Anzhen Road, Chaoyang District, Beijing 100029, China; [4]Department of Cardiovascular Medicine, Chinese PLA General Hospital & Chinese PLA Medical School, No.28 Fuxing Road, Haidian District, Beijing 100853, China; and [5]Department of Cardiology, Medical College of Soochow University, No.1 Shizi Road, Gusu District, Suzhou 215006, China

Received 20 February 2021; revised 13 May 2021; editorial decision 6 July 2021; accepted 15 July 2021; online publish-ahead-of-print 4 August 2021

See page 3800 for the editorial comment on this article (doi:10.1093/eurheartj/ehab515)

Aims 3′ untranslated region (3′ UTR) of mRNA is more conserved than other non-coding sequences in vertebrate genomes, and its sequence space has substantially expanded during the evolution of higher organisms, which substantiates their significance in biological regulation. However, the independent role of 3′ UTR in cardiovascular disease was largely unknown.

Methods and results Using bioinformatics, RNA fluorescent *in situ* hybridization and quantitative real-time polymerase chain reaction, we found that 3′ UTR and coding sequence regions of *Ckip-1* mRNA exhibited diverse expression and localization in cardiomyocytes. We generated cardiac-specific *Ckip-1* 3′ UTR overexpression mice under wild type and casein kinase 2 interacting protein-1 (CKIP-1) knockout background. Cardiac remodelling was assessed by histological, echocardiography, and molecular analyses at 4 weeks after transverse aortic constriction (TAC) surgery. The results showed that cardiac *Ckip-1* 3′ UTR significantly inhibited TAC-induced cardiac hypertrophy independent of CKIP-1 protein. To determine the mechanism of *Ckip-1* 3′ UTR in cardiac hypertrophy, we performed transcriptome and metabolomics analyses, RNA immunoprecipitation, biotin-based RNA pull-down, and reporter gene assays. We found that *Ckip-1* 3′ UTR promoted fatty acid metabolism through AMPK–PPARα–CPT1b axis, leading to its protection against pathological cardiac hypertrophy. Moreover, *Ckip-1* 3′ UTR RNA therapy using adeno-associated virus obviously alleviates cardiac hypertrophy and improves heart function.

Conclusions These findings disclose that *Ckip-1* 3′ UTR inhibits cardiac hypertrophy independently of its cognate protein. *Ckip-1* 3′ UTR is an effective RNA-based therapy tool for treating cardiac hypertrophy and heart failure.

* Corresponding authors. Tel: +86 135 52722709, Email: yingxianli@aliyun.com (Y.L.); Tel: +86 311 80786311, Email: chang7676@163.com (Y.-Z.C.); Tel:+86 133 11508172, Email: sh2ling@126.com (S.L.)

Graphical Abstract

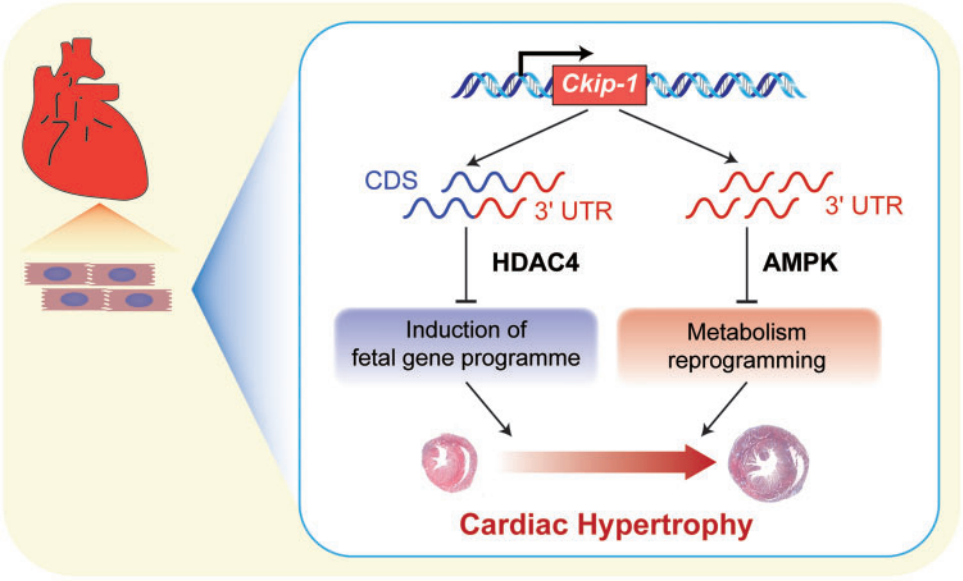

Ckip-1 gene plays an important role in fine-tuning cardiac hypertrophy through two ways mediated by 3′ UTR of mRNA and CKIP-1 protein.

Keywords Cardiac hypertrophy • CKIP-1 3′ UTR • AMPK • CaMKK2 • Fatty acid metabolism

Translational perspective

Cardiac remodelling is highly regulated both at the transcription and post-transcriptional processing. mRNA contains both the genetic information translated from coding regions, but also untranslated regions (UTRs) at their 5′ and 3′ ends. In this study, we disclose a totally novel function of *Ckip-1* 3′ UTR, which substantially inhibits pressure overload-induced pathological cardiac hypertrophy independent of CKIP-1 protein. Overexpression of *Ckip-1* 3′ UTR in cardiomyocytes substantially ameliorates metabolism reprogramming through AMPK–PPARα–CPT1b axis and promotes heart function. The findings demonstrated that *Ckip-1* 3′UTR RNA would be a potential effective RNA-based therapy tool for treating pathological cardiac hypertrophy.

Introduction

Pathological cardiac hypertrophy presents as the heart's response to a variety of external and internal stresses, including mechanical or neurohormonal stimuli, which eventually leads to heart failure (HF).[1–4] Cardiac hypertrophy is characterized by metabolic remodelling, Foetal gene reactivation, interstitial fibrosis, and contractile dysfunction.[5–8] To improve clinical outcomes and avoid HF, new therapies that target the precise regulatory mechanisms of cardiac hypertrophy are needed.

RNA molecules, including protein-coding mRNAs and non-coding RNAs, play critical roles in gene regulation. RNA metabolism is highly regulated and plays important roles in cardiac development and disease.[9–11] Various modification steps, including 5′-capping, intron splicing, and 3′-polyadenylation, are required to generate mature mRNAs. The structure of mRNA comprises a coding sequence (CDS) region and 5′ and 3′ untranslated regions (UTRs).[12,13] The central hubs of post-transcriptional regulation are located in the UTRs of mRNAs.[14–16] Regulatory elements that determine the fate of mRNAs, by regulating mRNA degradation, translation, and localization, are often located in the 3′ UTR. 3′ UTRs are highly conserved in vertebrate genomes, highlighting their significant biological roles.[17,18] Furthermore, 3′ UTRs are involved in the pathogenesis of various genetic diseases.[19] For example, an extended region of CTG repeats in the 3′ UTR of myotonic dystrophy protein kinase causes cardiac conduction defects in humans.[20] With such a protein-centric view, 3′ UTRs are typically defined by canonical transcription, showing that they are contiguous with the upstream coding regions in the mRNA. Initially, CDS and 3′ UTR of mRNA were thought to be one-to-one ratio correlates, but it was surprising to find widespread unbalanced expression and different subcellular localization in mammals, plants, and bacteria.[21,22] Genes with high 3′ UTR/CDS ratios are involved in neuron development.[23] Moreover, a protein-independent role of a 3′ UTR has been discovered in *Drosophila melanogaster*; transfection with the *Oskar* 3′ UTR rescues the eggless phenotype of *Oskar* mRNA-null mutants, independently of the Oskar protein.[24] However, the independent roles of 3′ UTR in cardiovascular disease are largely unknown.

A hallmark of energy metabolism in pathological hypertrophic growth is the downregulation of fatty acid (FA) oxidation and a significant increase in glycolysis.[25,26] With increasing severity of cardiac hypertrophy, the pathological heart undergoes dramatic reprogramming that is linked to handling of excess FA that arise from adipose tissue. This transition results in a cardiac metabolic signature that embraces FA overload.[27–29] The toxic intracellular accumulation of lipid species contributes to HF.[30,31] Understanding the metabolic remodelling in the hypertrophic heart fuel is critical for developing the concept of metabolic intervention in HF. AMP-activated protein kinase (AMPK) is a crucial energy sensor and a master regulator of cell metabolism that responds to a variety of stresses in the heart.[32] AMPK activation efficiently inhibited cardiac hypertrophy.[32,33] While we understand the basic regulation of AMPK activity by kinases, recent studies had introduced the concept that AMPK was regulated by non-coding RNA.[34] However, the role of 3′ UTRs in AMPK regulation is unclear.

In this study, we examined the alteration of mRNA 3′ UTR and CDS in the cardiac tissue of HF patients using publicly available high-throughput sequencing data. We found asymmetry in the expression levels of 3′ UTRs and their cognate CDS regions in HF patients; this effect was particularly prominent for casein kinase 2 interacting protein-1 (CKIP-1). Our previous study demonstrated that CKIP-1 protein was a novel regulator of cardiac remodelling via HDAC4/MEF2C pathway.[35] However, the physiological role of *Ckip-1* 3′ UTR in the heart is unknown.

Here, we identified *Ckip-1* 3′ UTR as a novel regulator of pressure overload-induced cardiac hypertrophy independently of CKIP-1 protein. Moreover, *Ckip-1* 3′ UTR promoted FA metabolism through AMPK–PPARα–CPT1b axis, which lead to protect against pathological cardiac hypertrophy. Notably, treatment with *Ckip-1* 3′ UTR sequences successfully alleviated cardiac hypertrophy and HF. Our findings suggest that the *Ckip-1* 3′ UTR performs a novel function in cardiovascular disease independently of its cognate protein (*Graphical abstract*).

Methods

Expanded methods are available in the Supplementary material online.

Results

The 3′ untranslated region and coding sequence regions of *Ckip-1* mRNA exhibit diverse expression and localization in heart

To systematically elucidate mRNA 3′ UTR and CDS expression during HF, we examined publicly available deep RNA-sequencing (RNA-seq) data that were generated from non-failing human heart (NF) and non-ischaemic failing human heart (NICM).[36] In comparison with the NF samples, the discordant expression changes in the CDS and 3′ UTR were observed in NICM samples (Supplementary material online, *Figure S1A*). Among the top 25 upregulated or downregulated significantly changed mRNA 3′ UTR or CDS from RNA-seq data (*Figure 1A and B* and Supplementary material online, *Tables S1* and *S2*), *CKIP-1*, which had been demonstrated to respond to pathological hypertrophy and promoted cardiac function in our previous studies,[35] attracted our attention. Notably, the expression of the 3′ UTR and CDS regions of *CKIP-1* mRNA in HF patient cardiac tissue was inconsistent. Quantitative real-time polymerase chain reaction (qRT-PCR) analysis revealed that the level of the *CKIP-1* mRNA 3′ UTR was significantly higher (four-fold) in HF samples compared with non-HF samples, while the level of the *CKIP-1* mRNA CDS was significantly lower (0.5-fold) in HF samples compared with non-HF samples (*Figure 1C and D* and Supplementary material online, *Table S3*).

In primary adult mouse cardiomyocytes, we next performed two-colour RNA *in situ* hybridization for *Ckip-1* mRNA 3′ UTR (green signal) and CDS (red signal) with Fam-labelled and Cy3-labelled RNA probes, respectively (*Figure 1E* and Supplementary material online, *Figure S1B*). Fam- and Cy3-labelled probes specific for 18S RNA were used as cytoplasmic markers and positive controls. A non-specific RNA probe was used as a negative control (Supplementary material online, *Figure S1C*). The results showed that *Ckip-1* mRNA 3′ UTR and CDS existed diverse cellular localization in the cardiomyocytes. Simultaneously, we monitored copies change of *Ckip-1* mRNA 3′ UTR and CDS in isolated cardiomyocytes. Absolute copy number analysis revealed that 3′ UTR was present at ∼4000 copies per cell; the CDS regions of *Ckip-1* mRNA showed a lower abundance of ∼870 copies per cell (*Figure 1F*). Our findings suggest that the abundance of the cardiac *Ckip-1* 3′ UTR was higher than that of *Ckip-1* CDS and that the *Ckip-1* 3′ UTR and CDS exhibited different spatial distributions in cardiomyocytes.

We further analysed *Ckip-1* mRNA 3′ UTR and CDS transcript levels in cardiac hypertrophy induced by transverse aortic constriction (TAC) in mice (*Figure 1G* and Supplementary material online, *Figure S1D*). Remarkably, *Ckip-1* CDS expression reached its peak level at Day 7 in comparison with the sham control, whereas 3′ UTR expression showed an initial increase 14 days after TAC, but it began to considerably decrease 21 days after TAC (*Figure 1G*). The results demonstrated that 3′ UTR and CDS regions of *Ckip-1* mRNA exhibit unequal expression change in response to HF.

Cardiac overexpression of *Ckip-1* 3′ untranslated region blunts transverse aortic constriction-induced cardiac hypertrophy

To explore the role of *Ckip-1* 3′ UTR in cardiac hypertrophy, we generated transgenic (TG) mice with overexpressing the *Ckip-1* 3′-UTR in cardiomyocytes under control of the α-MHC promoter (*Figure 2A*). Two independent lines of TG mice (TG1 and TG2) were established. Compared to wild-type (WT) mice, *Ckip-1* 3′ UTR mRNA levels of these two lines were increased four- to seven-fold (Supplementary material online, *Figure S2A and B*). We selected TG-2 mouse line that exhibited specific higher expression levels of *Ckip-1* 3′ UTR in heart tissues for subsequent experiments (Supplementary material online, *Figure S2C*). *Ckip-1* 3′ UTR TG mice and their age-matched WT littermate controls were subjected to cardiac pressure overload by TAC. After 4 weeks of TAC, we performed myocardial histology analysis to evaluate cardiomegaly and fibrosis (*Figure 2B and C*). We found a significant increase in cardiac fibrosis after TAC, which was decreased in 3′ UTR TG hearts compared with WT mice

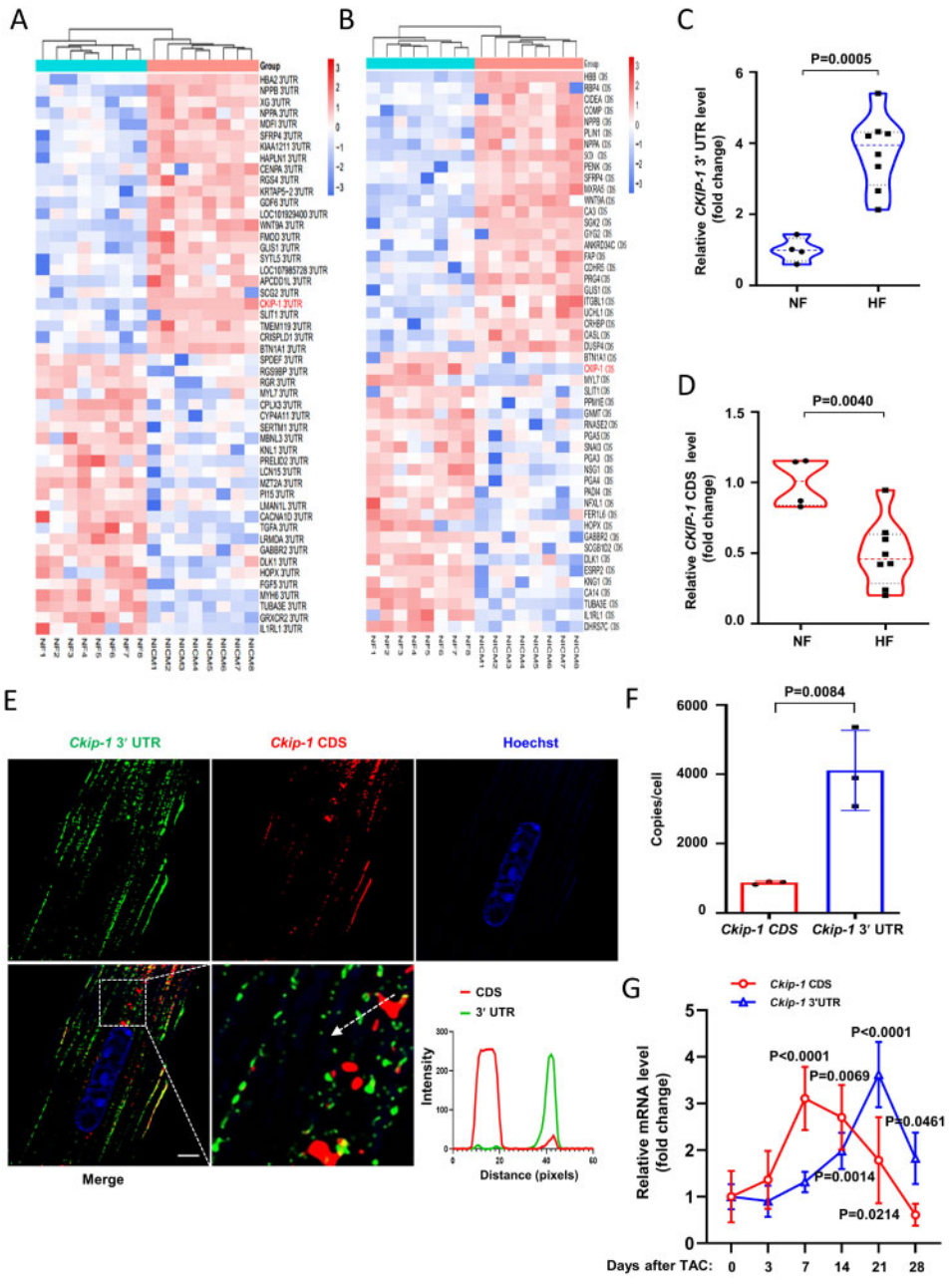

Figure 1 Expression and subcellular localization profile for *Ckip-1* 3′ untranslated region and coding sequence in heart. (*A*) Heat map analysis of mRNAs 3′ untranslated region that were differentially expressed between non-ischaemic human heart failing clinical samples and non-failing human heart clinical samples from RNA-seq data (>2.0-fold; $P < 0.05$; filtered to show the top 25 upregulated or downregulated results for mRNAs 3′ untranslated region). (*B*) Heat map was generated from mRNAs coding sequence differentially expressed in NICM clinical samples which included the top 25 downregulated (blue) and 25 upregulated (red) coding sequences. (*C* and *D*) Quantitative real-time polymerase chain reaction analysis of *CKIP-1* coding sequence (*C*) and 3′ untranslated region mRNA levels (*D*) in human hearts of non-failing and failure patients. Data are mean ± SD. (*E*) RNA fluorescent *in situ* hybridization (FISH) was conducted to detect expression of *Ckip-1* mRNA fragment using probes specific for 3′ untranslated region (green) or coding sequence (red) sequences in primary mouse cardiomyocytes. Line graphs of both fluorescence intensities showed subcellular localization along the entire length of the dashed line. Scale bar, 5 μm. (*F*) Quantitative analysis of *Ckip-1* 3′ untranslated region and coding sequence RNA copies per primary isolated adult mouse cardiomyocytes. Data are mean ± SD. (*G*) Eight- to 10-week-old male C57BL/6 mice were subjected to transverse aortic constriction. Hearts were harvested after 3, 7, 14, 21, and 28 days. Sham surgery was used as control. Time-course analysis of *Ckip-1* 3′ untranslated region and coding sequence mRNA levels during transverse aortic constriction surgery in wild-type mice hearts. *P*-value represents the comparison of transverse aortic constriction group at indicated time point and the corresponding control group. Data are mean ± SD. Statistical analysis for the comparison of two groups was performed using two-tailed unpaired Student's *t*-test. Statistical differences among groups were analysed by one-way ANOVA with Šídák *post hoc* test to determine group differences. Each statistical comparison undertaken has an assigned *P*-value (adjusted for multiplicity). Differences were considered significant at *P*-value <0.05. CDS, coding sequence; TAC, transverse aortic constriction; UTR, untranslated region.

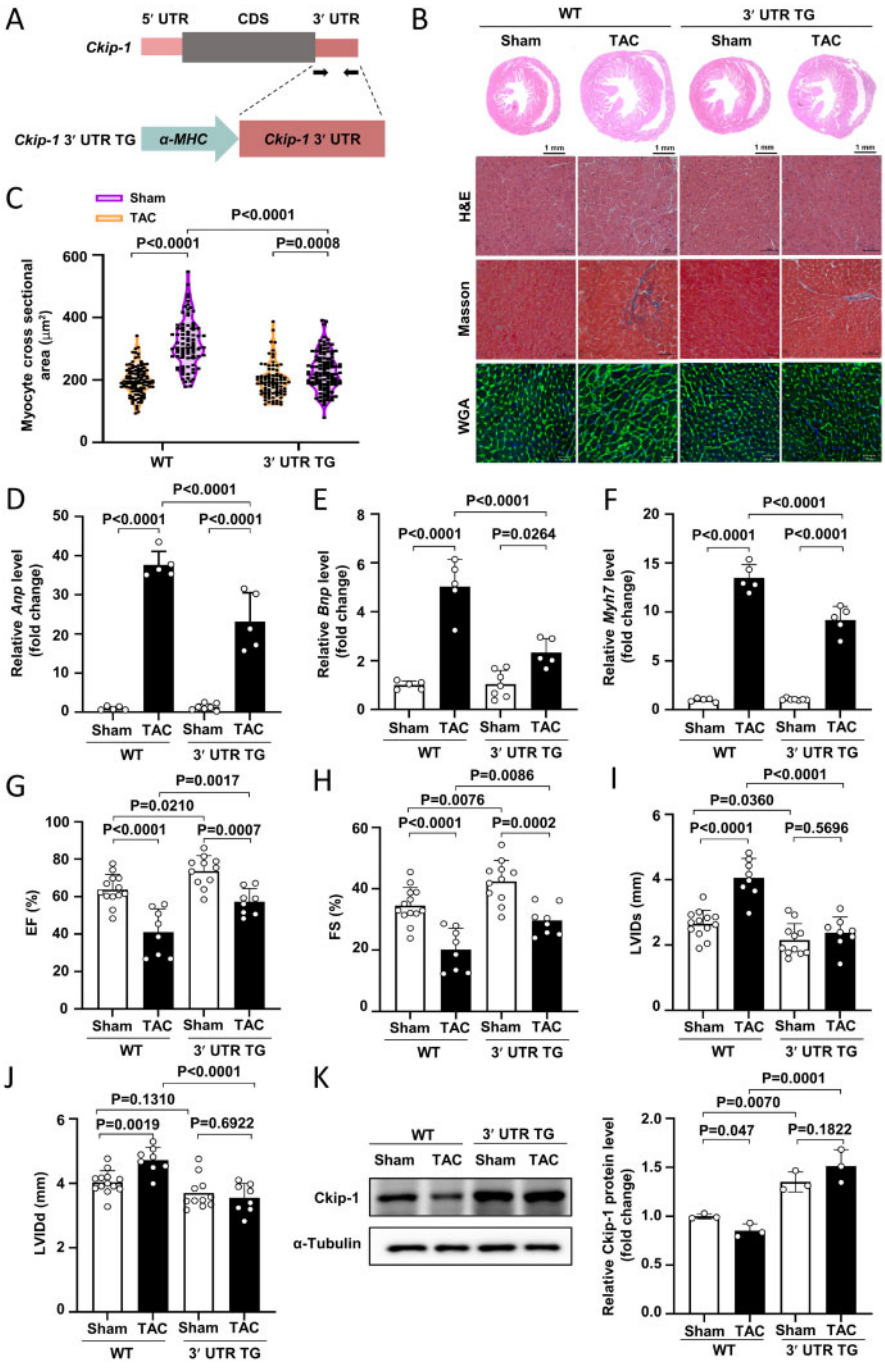

Figure 2 Overexpression of *Ckip-1* 3′ untranslated region in heart alleviates cardiac dysfunction. (*A*) Schematic illustration of cardiac-specific *Ckip-1* 3′ untranslated region transgenic (*Ckip-1* 3′ untranslated region transgenic) mouse lines. (*B* and *C*) Haematoxylin and eosin-stained cross-sections of hearts from sham- or transverse aortic constriction-operated wild-type or *Ckip-1* 3′ untranslated region transgenic mice show gross changes of cardiac hypertrophy (scale bar, 50 μm). Sections of hearts are stained with Masson trichrome to detect fibrosis (scale bar, 50 μm). Wheat germ agglutinin staining is used to demarcate cell boundaries (*C*) (scale bar, 20 μm). (*D–F*) Hypertrophic marker genes' (*Anp, Bnp*, and *Myh7*) expression levels were assessed as indicated. (*G–J*) Echocardiography showed ejection fraction (*G*), fractional shortening (*H*), end-systolic left ventricular internal diameter (*I*), and end-diastolic left ventricular internal diameter (*J*) in indicated groups. (*K*) Western blot analysis of CKIP-1 expression in total protein extracts from wild-type or *Ckip-1* 3′ untranslated region transgenic mice after sham or transverse aortic constriction surgery. Data are mean ± SD. Statistical differences among groups were analysed by two-way ANOVA with Šídák *post hoc* test to determine group differences. Each statistical comparison undertaken has an assigned *P*-value (adjusted for multiplicity). Differences were considered significant at *P*-value <0.05. CDS, coding sequence; EF, ejection fraction; FS, fractional shortening; H&E, haematoxylin and eosin; LVIDd, end-diastolic left ventricular internal diameter; LVIDs, end-systolic left ventricular internal diameter; TAC, transverse aortic constriction; TG, transgenic; UTR, untranslated region; WGA, wheat germ agglutinin; WT, wild-type.

(*Figure 2B* and Supplementary material online, *Figure S2D*). Staining with wheat germ agglutinin revealed that the cross-sectional area was significantly smaller in 3′ UTR TG hearts compared with WT hearts after TAC (*Figure 2C*). We found no significant difference between the heart weight/body weight ratios of *Ckip-1* 3′ UTR TG mice and WT mice after TAC (Supplementary material online, *Figure S2E*). At the molecular level, the TAC-induced expression of the hypertrophic markers, atrial natriuretic peptide (*Anp*), brain natriuretic peptide (*Bnp*), and myosin heavy chain 7 (*Myh7*), was significantly downregulated in 3′ UTR TG mice (*Figure 2D–F*).

Echocardiography was performed to monitor cardiac structural and functional changes. After TAC, WT mice represented impaired contractile function. By contrast, ejection fraction (EF) and fractional shortening (FS) after 28 days from sham or TAC surgery group were significantly increased in 3′ UTR TG mice compared with WT mice, indicating the benefits of *Ckip-1* 3′ UTR under basal and stress conditions (*Figure 2G and H*). This was accompanied in 3′ UTR TG mice by significantly decreased end-diastolic left ventricular internal diameter (LVIDd) and end-systolic left ventricular internal diameter (LVIDs; *Figure 2I and J*), and ventricular wall thickness was unchanged (Supplementary material online, *Figure S2F–I*). In addition, western blot analysis showed increased CKIP-1 protein levels in response to 3′ UTR overexpression (*Figure 2K*). These data suggested that *Ckip-1* 3′ UTR overexpression reduced the severity of cardiac hypertrophy after TAC.

To investigate the role of *Ckip-1* 3′ UTR in the regulation of physiological cardiac remodelling, we subjected *Ckip-1* 3′ UTR TG and WT mice to a 3-week swimming programme to induce physiological cardiac hypertrophy. The swimming exercise caused an increase in heart weight/body weight without cardiac fibrosis in WT and *Ckip-1* 3′ UTR TG mice (Supplementary material online, *Figure S3A and B*). Echocardiography revealed that cardiac function increased significantly after the swimming programme in both WT and *Ckip-1* 3′ UTR TG mice and that this effect was stronger in *Ckip-1* 3′ UTR TG mice compared with WT mice (Supplementary material online, *Figure S3C and D*). Cardiac structure data indicated that LVIDs was significantly decreased in 3′ UTR TG mice (Supplementary material online, *Figure S3E*), LVIDd and ventricular wall thickness was unchanged compared with WT mice (Supplementary material online, *Figure S3F–J*). These data suggested that *Ckip-1* 3′ UTR was also involved in the regulation of compensatory physiological changes induced by swimming.

Ckip-1 3′ untranslated region protects against adverse cardiac remodelling in a CKIP-1 protein-independent manner

To determine whether the role of *Ckip-1* 3′ UTR in cardiac hypertrophy is independent of its cognate CKIP-1 protein, we generated a *Ckip-1* 3′ UTR TG mouse line with a *Ckip-1* gene knockout (KO) genetic background (KO/3′ UTR TG) (*Figure 3A*). *Ckip-1* 3′ UTR was highly expressed in KO/3′ UTR TG, while no *Ckip-1* 3′ CDS and CKIP-1 proteins were detected (Supplementary material online, *Figure S4A–C*). KO and KO/3′ UTR TG littermates at 2 months of age underwent TAC surgery for 4 weeks. *Ckip-1* KO mice exhibited marked cardiac hypertrophy, as revealed by size enlargements, large areas of fibrosis, and increased heart weight/body weight (*Figure 3B–D*). In comparison with KO mice, KO/3′ UTR TG mice exhibited a decreased response to pressure overload-induced cardiac hypertrophy. The cardiomyocyte sizes and heart weight/body weight ratios of KO/3′ UTR TG mice were significantly decreased after TAC (*Figure 3C and D*). Masson trichrome staining revealed less fibrosis in the heart of KO/3′ UTR TG mice compared with KO mice (*Figure 3B* and Supplementary material online, *Figure S4D*). The expression levels of Foetal genes, *Anp*, *Bnp*, and *Myh7*, were lower in the KO/3′ UTR TG mice than in KO mice (*Figure 3E–G*).

Echocardiographic analysis showed significant decreases in EF and FS in KO mice, but no changes in KO/3′ UTR TG mice, after 4 weeks of TAC (*Figure 3H and I*). In KO mice, 4 weeks of TAC caused increases in LVIDs and LVIDd, and this response was markedly reduced in KO/3′ UTR TG mice (*Figure 3J and K*). There was similar cardiac ventricle wall thickness in KO/3′ UTR TG and KO mice (Supplementary material online, *Figure S4E–H*). When compared with age-matched WT mice group after TAC, the data of histology (Supplementary material online, *Figure S5A*), heart weight/body weight (Supplementary material online, *Figure S5B*), EF and FS (Supplementary material online, *Figure S5C and D*) demonstrated that *Ckip-1* KO was hypersensitive to pressure overload-induced cardiac hypertrophy and *Ckip-1* 3′ UTR TG mice under KO background were more resistant to pressure overload stress than that in KO mice.

Collectively, these results indicated that *Ckip-1* 3′ UTR reversed cardiac dysfunction and remodelling after TAC surgery independent of CKIP-1 protein.

Ckip-1 3′ untranslated region alters metabolic pathway gene expression profile

To investigate the potential mechanisms by which *Ckip-1* 3′ UTR mediated cardiac function, we performed RNA-seq and identified 705 upregulated and 462 downregulated genes in 3′ UTR TG cardiac tissue when compared to WT cardiac tissue (Supplementary material online, *Figure S6A*). Large-scale gene function analysis was performed with the gene ontology enrichment system, which revealed multiple significantly enriched biological processes, including long-chain FA metabolic process (Supplementary material online, *Figure S6B*). The Kyoto Encyclopedia of Genes and Genomes (KEGG) enrichment analysis data indicated the involvement of upregulated gene sets in energy metabolism-related pathways, including AMPK and peroxisome proliferator-activated receptor α (PPARα) pathways (Supplementary material online, *Figure S6C*). To investigate whether the role of *Ckip-1* 3′ UTR in the regulation of cardiac hypertrophy related pathway is independent of CKIP-1 protein, we performed RNA-seq in KO/3′ UTR TG and KO cardiac tissue and identified 817 upregulated and 968 downregulated genes in KO/3′ UTR TG cardiac tissue compared with the KO group (*Figure 4A*). Gene ontology analysis revealed multiple significantly enriched biological processes including lipid metabolic process and energy homeostasis, among which the changes in lipid metabolic were most significant (*Figure 4B*). The KEGG enrichment analysis data also indicated the involvement of upregulated gene sets in energy metabolism-related pathways, including AMPK and PPARα pathways (*Figure 4C*). Moreover, gene set enrichment analysis indicated that *Ckip-1* 3′ UTR exhibited a significant positive relationship with AMPK pathway (*Figure 4D*).

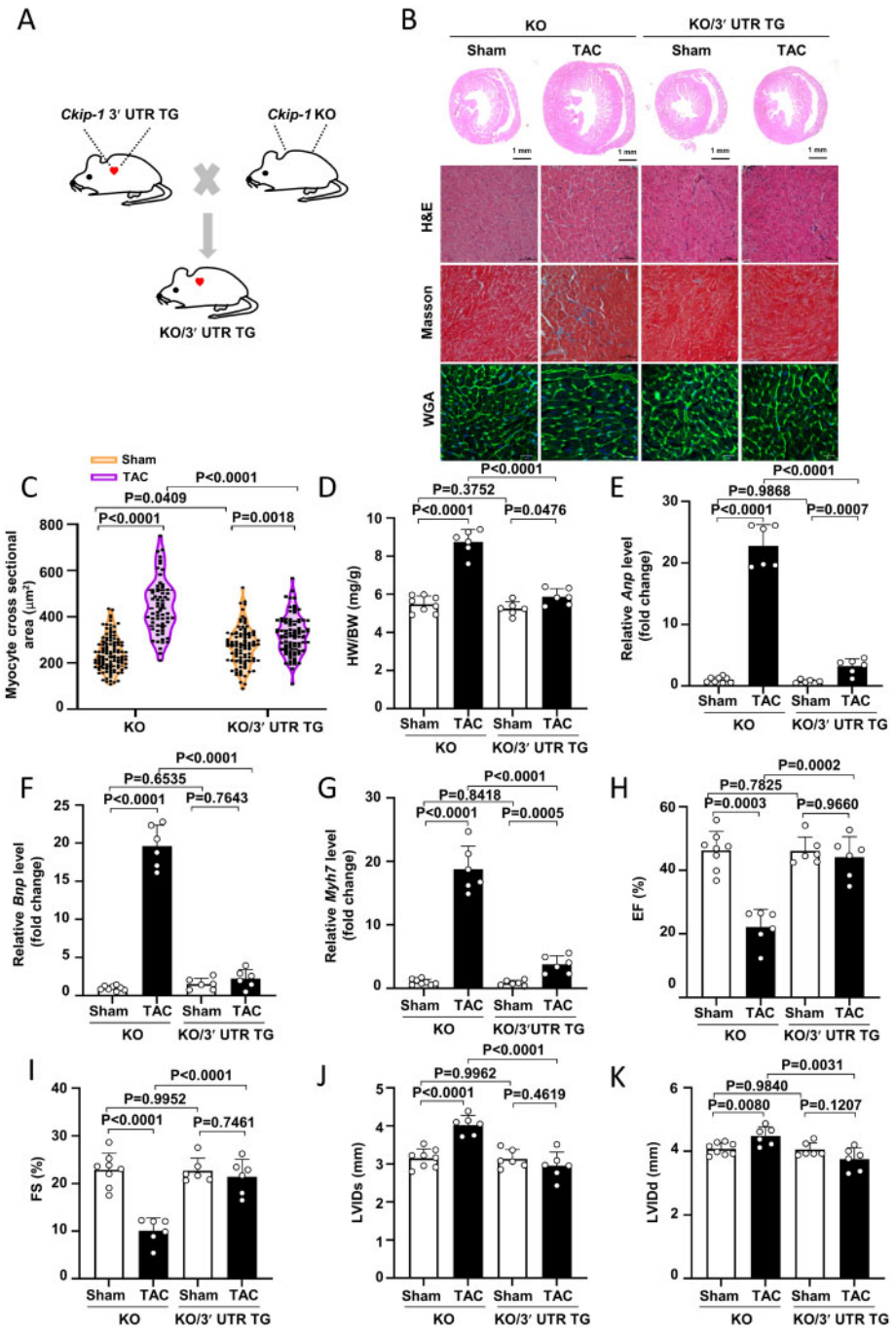

Figure 3 Cardiac-specific *Ckip-1* 3′ untranslated region overexpression in CKIP-1 knockout mice inhibit transverse aortic constriction-induced cardiac hypertrophy. (*A*) Generation of *Ckip-1* knockout/3′ untranslated region transgenic mice by crossing α-MHC-*Ckip-1* 3′ untranslated region transgenic mice with global loss of *Ckip-1* mice. (*B*) *Ckip-1* knockout/3′ untranslated region transgenic mice and *Ckip-1* knockout mice littermates were subjected to transverse aortic constriction or sham surgery. Representative images of heart sections stained with haematoxylin and eosin (scale bar, 50 μm), Masson trichrome (scale bar, 50 μm) and wheat germ agglutinin (scale bar, 20 μm) staining. (*C*) Quantitative analysis of the cross-sectional area of the cardiomyocytes shown in indicated groups. (*D*) Heart weight-to-body weight ratio of *Ckip-1* knockout/3′ untranslated region transgenic mice and *Ckip-1* knockout mice with transverse aortic constriction or sham surgery. (*E–G*) Transcript levels of the indicated genes (*Anp, Bnp*, and *Myh7*) in heart samples from the indicated groups. (*H–K*) Cardiac ejection fraction (*H*), fractional shortening (*I*), end-systolic left ventricular internal diameter (*J*), and end-diastolic left ventricular internal diameter (*K*) were measured by transthoracic echocardiography. Data are mean ± SD. Statistical differences among groups were analysed by two-way ANOVA with Šídák *post hoc* test to determine group differences. Each statistical comparison undertaken has an assigned *P*-value (adjusted for multiplicity). Differences were considered significant at *P*-value <0.05. EF, ejection fraction; FS, fractional shortening; HW/BW, heart weight-to-body weight ratio; LVIDd, end-diastolic left ventricular internal diameter; LVIDs, end-systolic left ventricular internal diameter; KO, knockout; TAC, transverse aortic constriction; TG, transgenic; UTR, untranslated region.

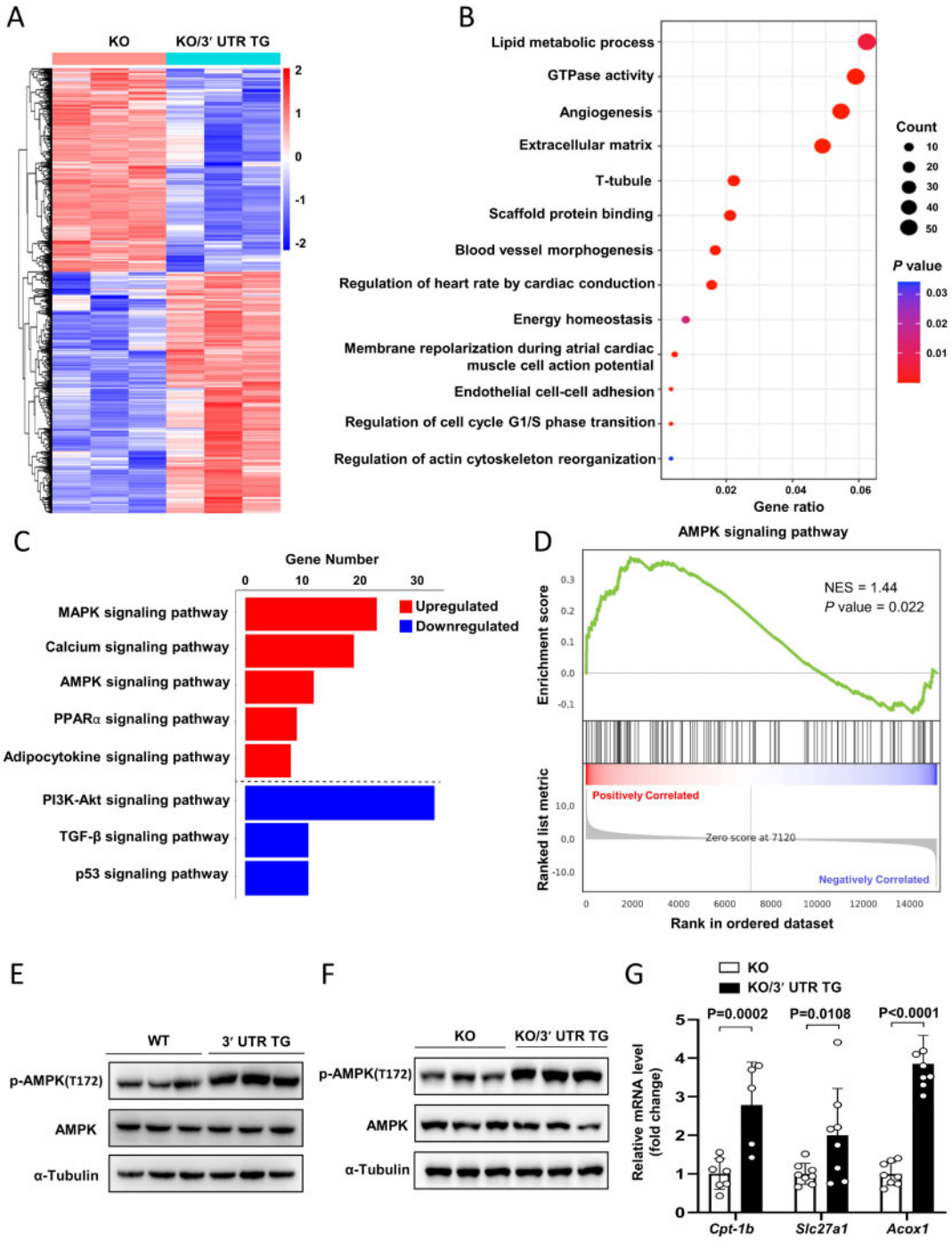

Figure 4 Transcriptome profile of *Ckip-1* knockout and *Ckip-1* knockout/3′ untranslated region transgenic mouse hearts. (*A*) Heat map of differentially expressed genes in *Ckip-1* knockout and *Ckip-1* knockout/3′ untranslated region transgenic mouse hearts using data generated by RNA-sequencing that were analysed with cut-off values of ± two-fold change and *P*-value <0.05. Red indicates high expression; blue indicates low expression. (*B*) A cluster profiler identified the 13 most significantly enriched gene ontology biological processes (fold change >2; adjusted $P < 0.05$). (*C*) KEGG pathway enrichment analysis of the identified differentially expressed genes that are upregulated (red) or downregulated (blue) in hearts. (*D*) Gene set enrichment analysis of AMPK signalling pathway. (*E*) Western blot showing the data of phospho-AMPK and total protein expression levels of AMPK in *Ckip-1* knockout and *Ckip-1* knockout/3′ untranslated region transgenic mice. α-Tubulin was used as loading control. (*F*) Western blot analysis of phospho-AMPK and total AMPK protein in heart extracts from wild-type and *Ckip-1* 3′ untranslated region transgenic mice. (*G*) Quantitative real-time polymerase chain reaction validation expression of genes related to lipid metabolism in the hearts between *Ckip-1* knockout and *Ckip-1* knockout/3′ untranslated region transgenic mice. Data are mean ± SD. Statistical analysis for comparison of two groups was performed using two-tailed unpaired Student's *t*-test. Differences were considered significant at *P*-value <0.05. KO, knockout; NES, normalized enrichment score; TG, transgenic; UTR, untranslated region.

Next, we then evaluated whether *Ckip-1* 3′ UTR regulated AMPK activity. The results showed that *Ckip-1* 3′ UTR TG mice resulted in a large increase in T172-phosphorylated AMPKα compared with WT mice, whereas the total AMPK protein remained unchanged (*Figure 4E*). Moreover, AMPKα was significantly activated in KO/3′ UTR TG mice compared with KO mice, independent of CKIP-1 protein (*Figure 4F*). AMPK activation increases PPARα expression and subsequently induced its targets transcription, which involved in FA transport and FA oxidation, including long-chain FA transport protein 1 (*Slc27a1*), carnitine palmitoyltransferase1b (*Cpt-1b*), and acyl-coenzyme A oxidase 1 (*Acox1*). Their expression levels were further confirmed by qRT-PCR (*Figure 4G*). Moreover, we investigated the oxygen consumption rate (OCR) in mitochondria isolated from heart tissues of *Ckip-1* 3′ UTR TG mice (under the background of WT or KO mice) (Supplementary material online, *Figure S6D–G*). The results demonstrated that cardiac-specific *Ckip-1* 3′ UTR overexpression whether in WT or *Ckip-1* KO mice could significantly increase the OCR of cardiac mitochondria compared with their controls, respectively (Supplementary material online, *Figure S6D–G*). Taken together, these data implicated that *Ckip-1* 3′ UTR regulated cardiac lipid metabolism through the AMPK–PPARα axis in the heart.

Ckip-1 3′ untranslated region promotes lipid metabolism and ATP synthesis during cardiac hypertrophy

To investigate the regulation of *Ckip-1* 3′ UTR on lipid metabolism during cardiac hypertrophy, we performed liquid chromatography–mass spectrometry- (*Figure 5A–C*) and gas chromatography–mass spectrometry-based targeted metabolomics analysis (*Figure 5D–E*) and metabolite quantification in the hearts of KO and KO/3′ UTR TG mice after TAC. Free FA levels were significantly lower in the cardiac tissue of KO/3′ UTR TG mice after TAC compared with KO mice (*Figure 5B and C*), while TCA cycle intermediates were increased from KO/3′ UTR TG mice in response to TAC (*Figure 5E*).

Next, we measured adenosine triphosphate (ATP) levels in KO and KO/3′ UTR TG mice after TAC surgery. ATP production increased in KO/3′ UTR TG mice but decreased in *Ckip-1* KO mice, after TAC (*Figure 5F*). Lipid accumulation was determined histologically by staining cardiac tissue sections with oil red O, which was markedly increased in sections from the hearts of KO mice but not in KO/3′ UTR TG mice (*Figure 5G* and Supplementary material online, *Figure S7*). Together, these data suggest that overexpression of *Ckip-1* 3′ UTR inhibited lipid accumulation and facilitated the generation of ATP through TCA cycle reactions from FA.

Ckip-1 3′ untranslated region acts as Let-7f sponge to facilitate the activation of CaMKK2–AMPK–PPARα axis

3′ UTRs often contain binding sites for regulatory miRNAs. Therefore, we investigated potential miRNA-based mechanisms driving AMPK regulation by the *Ckip-1* 3′-UTR. Bioinformatics analysis using TargetScan programme (Release 7.1) showed that both *Ckip-1* 3′ UTR and calcium/calmodulin-dependent kinase kinase 2 (*Camkk2*) 3′ UTR contained Let-7f targeting sites (*Figure 6A*). Notably, *Ckip-1* 3′ UTR overexpression increased the protein levels of CaMKK2 protein (*Figure 6B*), which directly phosphorylates AMPK at Thr172.[37] To verify whether Let-7f was involved in the regulation of *Ckip-1* 3′ UTR on CaMKK2, we examined the relationship between CaMKK2 and Let-7f. The results showed that knockdown of endogenous Let-7f induced an increase in CaMKK2 protein level, and Let-7f overexpression significantly reduced the level of CaMKK2 (*Figure 6C* and Supplementary material online, *Figure S8A*), but mRNA levels were not affected (Supplementary material online, *Figure S8B*). Moreover, the reporter gene activity of *Camkk2* 3′ UTR was inhibited by Let-7f, and mutation of Let-7f-binding sites in the *Camkk2* 3′ UTR abolished the inhibitory effect of Let-7f (*Figure 6D*). Furthermore, such an effect had not existed in other putative binding sites at positions 1191–1196 (Supplementary material online, *Figure S8C and D*). These results indicated that CaMKK2 protein level was regulated by Let-7f.

Next, we investigated whether *Ckip-1* 3′ UTR sequence could sponge Let-7f. Luciferase assay revealed that Let-7f could also suppress the luciferase activity of *Ckip-1* 3′ UTR, but it had less effect on the Let-7f-binding site mutation form of *Ckip-1* 3′ UTR (*Figure 6E*). To examine the interaction between *Ckip-1* 3′ UTR and Let-7f, we performed an RNA immunoprecipitation assay with anti-YFP antibody, determining whether Let-7f could be pulled down by the YFP-MS2-tagged *Ckip-1* 3′ UTR. Let-7f was significantly enriched by the YFP antibody, compared with the non-specific immunoglobulin G control antibody (*Figure 6F*). Then, we applied inverse pull-down assay to test whether Let-7f could enrich *Ckip-1* 3′ UTR using biotin-labelled specific Let-7f probe. The results showed that *Ckip-1* 3′ UTR but not its mutant was co-precipitated (*Figure 6G*). These results revealed that *Ckip-1* 3′ UTR directly interacted with Let-7f.

More importantly, overexpression of *Ckip-1* 3′ UTR but not *Ckip-1* 3′ UTR-mut increased CaMKK2 protein level, by which the phosphorylation of AMPK was also increased accordingly. Knockdown of Let-7f counteracted the regulation of *Ckip-1* 3′ UTR on CaMKK2 and the phosphorylation of AMPK (*Figure 6H* and Supplementary material online, *Figure S8E and F*). *In vivo*, the enhanced cardiac lipid metabolism induced by the overexpression of *Ckip-1* 3′ UTR was supported by increased expression of CaMKK2 and activation of AMPK. PPARα, the downstream regulator of AMPK, and PPARα-targeted gene CPT1b was also markedly upregulated in KO/3′ UTR TG mice compared with KO mice after TAC (*Figure 6I* and Supplementary material online, *Figure S8G–J*). Taken together, these results showed that *Ckip-1* 3′ UTR functions as an endogenous Let-7f sponge to sequester and inhibit Let-7f, resulting in the increase of CaMKK2 expression and AMPK activity. These events involved in the regulation of *Ckip-1* 3′ UTR on cardiac lipid metabolism.

Ckip-1 3′ untranslated region RNA therapy restricts cardiac hypertrophy and improves heart function

To further examine the therapeutic potential of *Ckip-1* 3′ UTR, we engineered an adeno-associated virus (AAV) vector to overexpress the *Ckip-1* 3′ UTR under control of the cardiomyocyte-specific cardiac troponin (*cTnT*) promoter. Mice were injected with 10^{12} AAV9-3′ UTR viral particles at 1 week after TAC surgery. After 3 weeks, cardiac function was analysed (*Figure 7A*). Injection of AAV9-3′ UTR led to approximately five-fold increase in *Ckip-1* 3′ UTR levels in heart (*Figure 7B*). In comparison with AAV9-control injected mice, mice injected with AAV9-3′ UTR exhibited a reduced hypertrophic

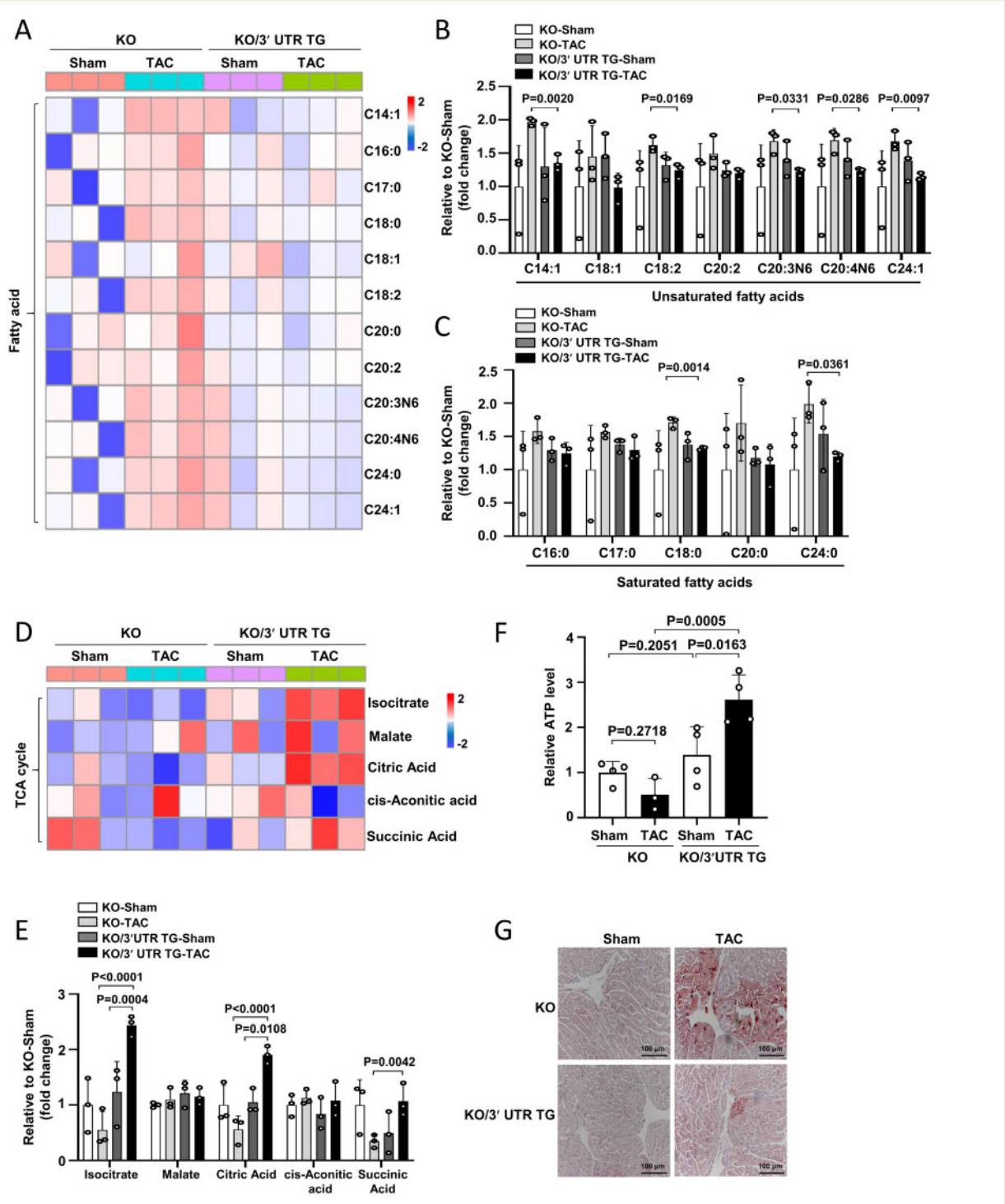

Figure 5 Metabolomics profile of *Ckip-1* knockout and *Ckip-1* knockout/3′ untranslated region transgenic mice during cardiac hypertrophy. (*A*) Heat map of metabolites associated with free fatty acids in the hearts of *Ckip-1* knockout and *Ckip-1* knockout/3′ untranslated region transgenic mice after transverse aortic constriction surgery, measured by metabolomics. (*B* and *C*) Quantification of free fatty acid (saturated fatty acid and unsaturated fatty acid) levels. (*D*) The heat map showing tricarboxylic acid intermediates in the heart samples obtained from *Ckip-1* knockout and *Ckip-1* knockout/3′ untranslated region transgenic mice after transverse aortic constriction surgery. (*E*) Histograms depicting myocardial tricarboxylic acid intermediates in the hearts of *Ckip-1* knockout and *Ckip-1* knockout/3′ untranslated region transgenic mice in response to transverse aortic constriction. (*F*) Intracellular ATP content of *Ckip-1* knockout/3′ untranslated region transgenic and *Ckip-1* knockout mice with transverse aortic constriction surgery. (*G*) Representative images of oil red O-stained sections in the hearts. Scale bar, 100 μm. Data are mean ± SD. Statistical differences among groups were analysed by two-way ANOVA with Šídák *post hoc* test to determine group differences. Each statistical comparison undertaken has an assigned *P*-value (adjusted for multiplicity). Differences were considered significant at *P*-value <0.05. ATP, Adenosine Triphosphate; KO, knockout; TAC, transverse aortic constriction; TG, transgenic; UTR, untranslated region.

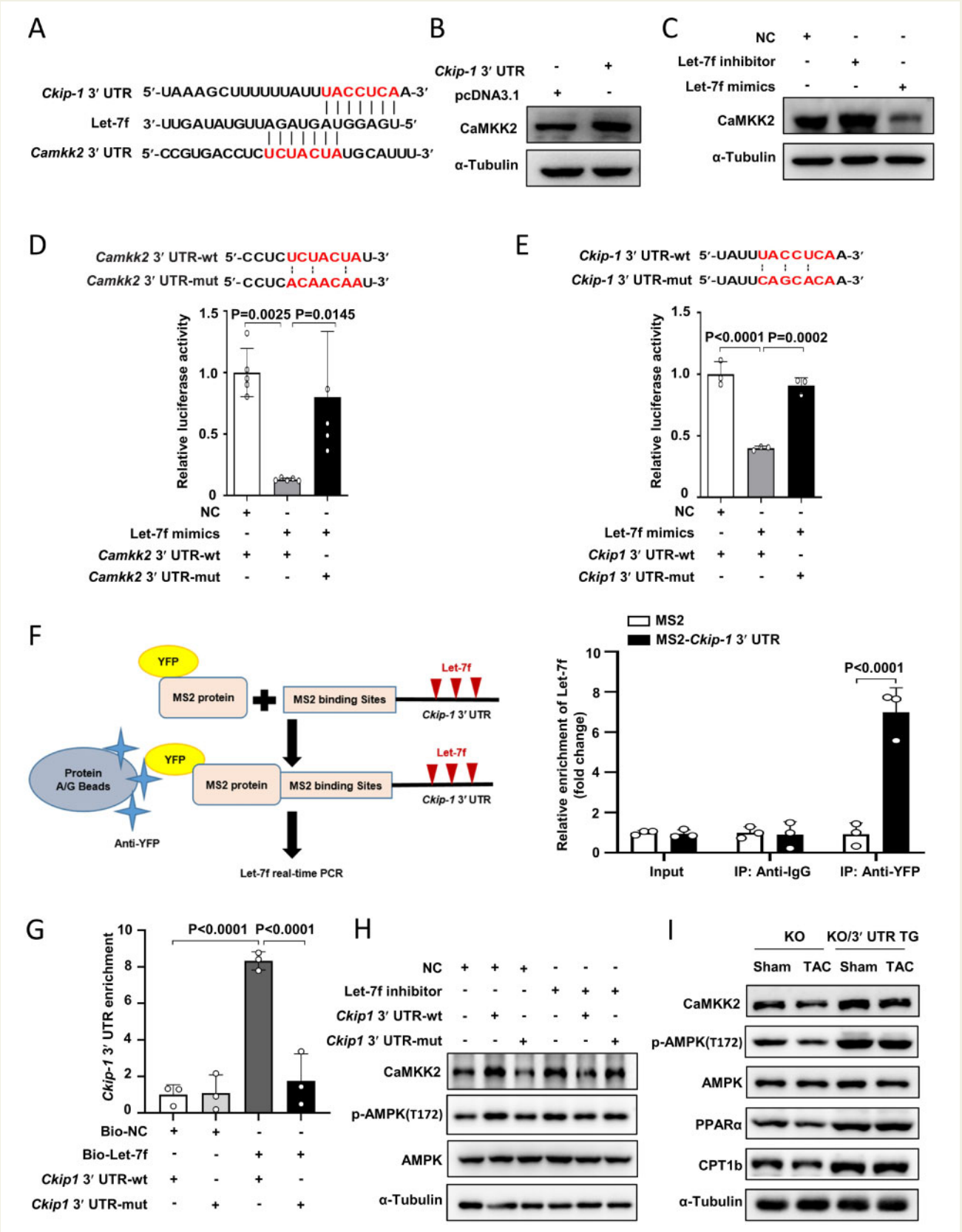

Figure 6 *Ckip-1* 3′ untranslated region regulates CaMKK2 protein levels by sponging Let-7f. (*A*) The predicted binding sites of Let-7f in *Ckip-1* 3′ untranslated region and *Camkk2* 3′ untranslated region were shown. (*B*) Western blot analysis of the CaMKK2 protein level in HEK293T cells after transfection with *Ckip-1* 3′ untranslated region or its control. (*C*) CaMKK2 protein expression in HEK293T cells transfected with negative control, Let-7f inhibitor, or Let-7f mimics. (*D*) Luciferase reporter of chimeric vectors carrying luciferase gene and a fragment of wild-type (wt) or mutant

Continued

response to TAC (*Figure 7C and D*). The heart weight/body weight ratios after TAC were significantly lower in mice injected with AAV9-3′ UTR compared with those injected with the AAV9 control (*Figure 7C*). Masson trichrome staining revealed less cardiac fibrosis in the cardiac tissue of AAV9-3′ UTR-injected mice after TAC compared with control mice after TAC (*Figure 7D* and Supplementary material online, *Figure S9A*). The reactivation of Foetal genes, *Anp, Bnp*, and *Myh7*, was evidently reduced in the AAV9-3′ UTR hearts in comparison with that in the AAV9-control hearts (*Figure 7E–G*). Echocardiographic analysis showed significant decreases in EF and FS in AAV9-control injected mice after 4 weeks of TAC, whereas the changes in AAV9-3′ UTR mice are not apparent (*Figure 7H and I*). Notably, intramyocardial lipid accumulation was clearly decreased in AAV9-3′ UTR-injected mice after TAC surgery (*Figure 7D* and Supplementary material online, *Figure S9B*). The expression of CaMKK2 and the activation of AMPK were significantly higher in the cardiac tissue of AAV9-3′-UTR-injected mice compared with AA9V control mice after TAC (*Figure 7J*). Moreover, cellular ATP production was higher after TAC in mice injected with the AAV9-3′-UTR compared with the AAV9 control (*Figure 7K*). These results demonstrated that *Ckip-1* 3′ UTR sequence represented a potential RNA-based therapy for treating cardiac hypertrophy and HF.

Discussion

In this study, we discovered a novel function of 3′ UTR independent of its cognate protein in the pressure overload-induced cardiac hypertrophy. First, we found that 3′ UTR and CDS regions of *Ckip-1* mRNA existed diverse expression and localization in cardiomyocytes. Cardiac-specific *Ckip-1* 3′ UTR overexpression in WT and *Ckip-1* KO mice protects from pressure overload-induced cardiac hypertrophy and HF. *Ckip-1* 3′ UTR functions as a novel regulator of cardiac hypertrophy independent of CKIP-1 protein. Meanwhile, integrated analysis of transcriptomics and metabolomics data revealed the important role of *Ckip-1* 3′ UTR in the regulation of AMPK signalling and cardiac metabolism. *Ckip-1* 3′ UTR significantly increased the phosphorylation of AMPK at Thr172 by targeting Let-7f and CaMKK2, activated the AMPK–PPARα–CPT1b axis, and promoted the lipid metabolism and ATP production during pathological cardiac hypertrophy. Importantly, *Ckip-1* 3′ UTR therapy significantly alleviated pressure overload-induced cardiac hypertrophy. Our results showed that *Ckip-1* 3′ UTR contained additional genetic information that conferred a protective role during maladaptive cardiac stress and metabolic remodelling, independently of CKIP-1 protein (*Figure 7L*).

3′ UTRs are the non-coding regions of mRNA. The median length of 3′ UTRs is approximately 10-fold higher in humans compared with yeast; however, the median length of CDSs is similar between the two species. This suggests a critical role of 3′ UTRs in higher organisms.[38] The activation of pathological stress responses requires extensive reprogramming of the 3′ UTR landscape. A growing number of studies have found that 3′ UTR-mediated processes are involved in the pathogenesis of various diseases, including myotonic dystrophy, β-thalassemia, thrombophilia, and cancer, as well as viral infections.[39–42] Large-scale unbiased analyses revealed dynamic mRNA 3′ UTR formation in the failing human heart.[43] However, the role of 3′ UTR in cardiac hypertrophy and HF was poorly understood. Our findings highlight a novel regulatory model involving *Ckip-1* 3′ UTR at the transcriptional level. The *Ckip-1* 3′ UTR restricts cardiac hypertrophy and improves heart function by regulating energy metabolism.

The central dogma of molecular biology implies that 3′ UTRs are typically contiguous with the upstream coding regions in the mRNA. Intriguingly, widespread differential expression between coding region and 3′ UTR sequences has been detected in neurons and other tissues.[21–23] 3′ UTR sequences have sophisticated functions, such as acting as scaffolds and mediating protein–protein interactions.[44] The length of 3′ UTR length is regulated by alternative cleavage and polyadenylation.[45] RNA-binding motif protein 10 is an anti-hypertrophy mediator that regulates the procession of 3′ UTR of key hypertrophy factors to regulate cardiac hypertroph.[46] A well-characterized model of a 3′ UTR that functions independently of its cognate CDS is the 3′ UTR of the *C. elegans* protein X-box binding protein 1 (*xbp-1*). The *xbp-1* transcript functions as part of a dual output *xbp-1* mRNA stress response axis.[47] In plants, ectopic expression of EBF1/2 3′ UTR fragment mediates Arabidopsis ethylene insensitivity.[48] However, in cardiovascular disease,

Figure 6 Continued
(mut) *Camkk2* 3′ untranslated region. Relative luciferase activity in HEK293T cells infected with negative control or Let-7f mimics and indicated luciferase reporter vectors. Data are mean ± SD. (*E*) *Ckip-1* wild-type 3′ untranslated region and a mutated 3′ untranslated region in the Let-7f-binding site were shown. Luciferase assay to validate the binding of Let-7f to *Ckip-1* 3′ untranslated region. (*F*) Left, the schematic diagram of MS2-based RNA immunoprecipitation assay. Right, quantitative real-time polymerase chain reaction was performed within RNA immunoprecipitation samples from HEK293T cells transfected with pcDNA3.1–12xMS2 (control vector), pcDNA3.1-*Ckip-1* 3′ untranslated region-12xMS2, or YFP-MS2. Data are mean ± SD. (*G*) The biotinylated Let-7f or negative control was transfected into HEK293T cells. Enrichment of *Ckip-1* 3′ untranslated region was assessed by biotin-based pull-down assay. Data are mean ± SD. (*H*) Silencing of Let-7f attenuates the increasement of target protein levels induced by forced expression of *Ckip-1* 3′ untranslated region. HEK293T was transfected with wild-type (wt) or mutant (mut) *Ckip-1* 3′ untranslated region and then co-transfected with negative control or Let-7f inhibitor for 48 h. Indicated target protein levels were detected by western blot. (*I*) Western blotting images summarized the expression levels of CaMKK2, phosphorylated AMPK, AMPK, PPARα, and CPT1b in hearts from *Ckip-1* knockout and knockout/*Ckip-1* 3′ untranslated region mice after transverse aortic constriction. Data are mean ± SD. Statistical analysis for comparison of two groups was performed using two-tailed unpaired Student's *t*-test. Statistical differences among groups were analysed by one-way ANOVA with Šídák *post hoc* test to determine group differences. Each statistical comparison undertaken has an assigned *P*-value (adjusted for multiplicity). Differences were considered significant at *P*-value <0.05. KO, knockout; NC, negative control; TAC, transverse aortic constriction; TG, transgenic; UTR, untranslated region.

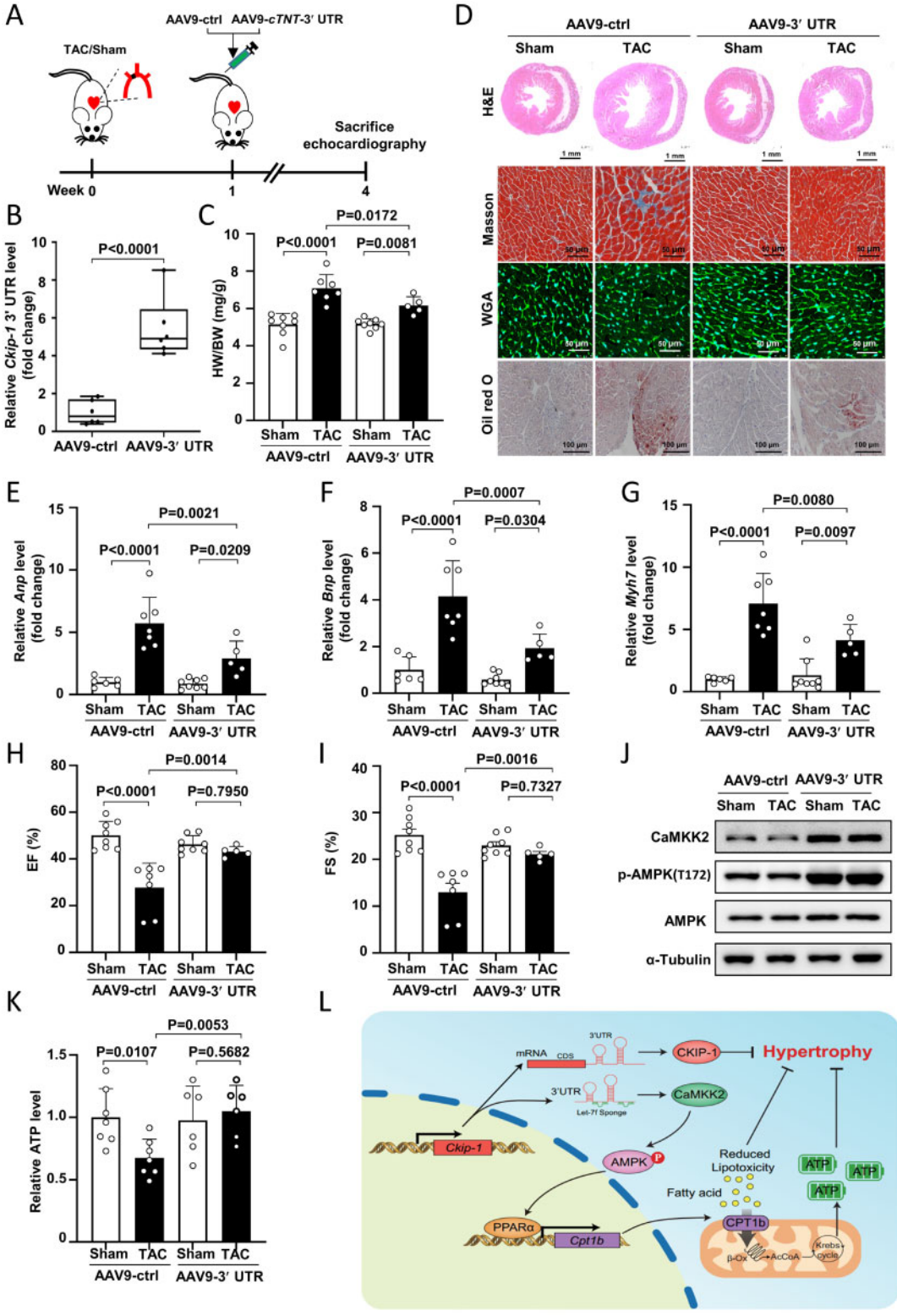

Figure 7 Therapeutic potential of *Ckip-1* 3′ untranslated region treatment in cardiac hypertrophy. (*A*) Study outline of AAV9-mediated overexpression experiment: 1 week after induction of cardiac hypertrophy via transverse aortic constriction surgery, wild-type mice were injected with either AAV9-*Ckip-1* 3′ untranslated region (AAV9-3′ untranslated region) or AAV9-control (AAV9-ctrl) (both under the control of a TnT promoter). (*B*) *Ckip-1* 3′ untranslated region mRNA expression level in heart extracts measured by quantitative real-time polymerase chain reaction (AAV9-ctrl and AAV9-*Ckip-1* 3′ untranslated region). Data are mean ± SD. (*C*) Heart tissue collection was performed at 4 weeks after surgery. Calculated heart weight-to-body weight ratios in Sham-AAV9-ctrl, transverse aortic constriction-AAV9-ctrl, Sham-AAV9-3′ untranslated region, and transverse aortic

Continued

independent roles of 3′ UTRs are largely unknown. In the present study, we found that 3′ UTR and CDS of *Ckip-1* exhibited different expression and non-uniform distribution patterns in cardiomyocytes. Notably, cardiac-specific *Ckip-1* 3′ UTR overexpression protected from pressure overload-induced cardiac hypertrophy and metabolic remodelling independently of CKIP-1 protein. To our knowledge, this is the first study to examine the role of 3′ UTR in cardiovascular disease independent of its cognate protein *in vivo*.

Phosphorylation of the Thr172 site of AMPK markedly increases its activity and is regulated by the liver kinase B1 or CaMKK2.[37] Genetic KO of *CaMKK2* in the cardiac tissues exacerbates ischaemic injury through CaMKK2–AMPK-dependent pathway.[49] AMPK activation also directly regulates transcription factor PPARα, which serves an important role in the regulation of cardiac lipid and energy metabolism.[50,51] In addition, PPARα promotes FA oxidation in cardiomyocytes via CPT1b, which is involved in the activation and transport of FA into mitochondria.[52]

CKIP-1 was initially identified as a specific CK2α subunit-interacting protein. CKIP-1 exhibits multiple biological functions in cardiovascular disease, bone formation, tumorigenesis, and immune regulation by interacting with various proteins.[53] In our previous study, we found that CKIP-1 conferred cardioprotective effects in various cardiac remodelling phenotypes.[35,54] The regulatory mechanism of CKIP-1 signalling pathway in the regulation of cardiac hypertrophy is dependent on the interaction of HDAC4 and PP2A.[33] Here, we describe a CKIP-1 protein-independent function of *Ckip-1* 3′ UTR as an endogenous Let-7f sponge that increases myocardial CaMKK2 expression after TAC stimulation. Subsequently, CaMKK2 induces AMPK activation and its downstream target PPARα. During hypertrophy, *Ckip-1* 3′ UTR maintains mitochondrial oxidative energy metabolism by redirecting FA trafficking to mitochondrion via CPT-1b activation. Our finding indicated that *Ckip-1* 3′ UTR enhances the role of the CaMKK2/AMPK/PPARα/CPT-1b pathway involved in cardiac energetics and mitigates cardiac lipotoxicity, thereby reversing the development of HF. Our findings demonstrated dual roles of *Ckip-1* 3′ UTR and CDS region regulation of cardiac hypertrophy and HF.

In summary, our findings enhance the current understanding of 3′ UTRs and their role in regulating cardiac hypertrophy. The single *Ckip-1* mRNA generates two distinct pathways that can allow cardiomyocytes to fine-tune their response to cardiac hypertrophy. This work reveals a novel model of 3′ UTRs-mediated regulation of cardiac hypertrophy and HF. Therefore, 3′ UTR represents an attractive RNA therapy tool for developing targeted therapeutic modalities for the treatment of cardiovascular disease.

Supplementary material

Supplementary material is available at *European Heart Journal* online.

Acknowledgements

We would like to thank H. P. Cheng and Xianhua Wang from Peking University for providing help in the measurement of mitochondrial respiratory function. We thank Shuoguo Li from Center for Biological Imaging (CBI), Institute of Biophysics, Chinese Academy of Science, for her help of taking and analysing fluorescence imaging.

Funding

This work was supported by the National Natural Science Foundation of China (81822026, 31670865, 31630038, and 81830061) and the Grant of State Key Lab of Space Medicine Fundamentals and Application (SMFA19A02, SMFA17B05, and SMFA19B03).

Conflict of interest: The authors declare no competing interests.

Data availability

The data underlying this article will be shared on reasonable request to the corresponding author.

References

1. Hill JA, Olson EN. Cardiac plasticity. *N Engl J Med* 2008;**358**:1370–1380.
2. Mosqueira D, Smith JGW, Bhagwan JR, Denning C. Modeling hypertrophic cardiomyopathy: mechanistic insights and pharmacological intervention. *Trends Mol Med* 2019;**25**:775–790.
3. Kim GH, Uriel N, Burkhoff D. Reverse remodelling and myocardial recovery in heart failure. *Nat Rev Cardiol* 2018;**15**:83–96.
4. Priori SG, Blomstrom-Lundqvist C, Mazzanti A, Blom N, Borggrefe M, Camm J, Elliott PM, Fitzsimons D, Hatala R, Hindricks G, Kirchhof P, Kjeldsen K, Kuck KH, Hernandez-Madrid A, Nikolaou N, Norekval TM, Spaulding C, Van Veldhuisen

Figure 7 Continued

constriction-AAV9-3′ untranslated region mice. (*D*) Representative images of gross morphology by haematoxylin and eosin (scale bar, 1 mm), Masson Trichrome (scale bar, 50 μm), wheat germ agglutinin (scale bar, 50 μm), and oil red O (scale bar, 100 μm) staining from the indicated groups. (*E–G*) *Anp*, *Bnp*, and *Myh7* mRNA expressions in heart tissue from the indicated groups. (*H* and *I*) Representative echocardiographic M-mode images, ejection fraction, and fractional shortening evaluated by echocardiography in the indicated groups. (*J*) Representative western blot of CaMKK2, phospho-AMPK, and total AMPK protein in cardiac tissue lysates from mice injected with 10^{12} AAV9-ctrl or AAV9-*Ckip-1* 3′ untranslated region and induced by transverse aortic constriction surgery during 4 weeks. Data are mean ± SD. (*K*) Measurement of myocardial ATP levels from the indicated groups. Data are mean ± SD. (*L*) Schematic illustration of *Ckip-1* 3′ untranslated region-regulated cardiac function and metabolic homeostasis. *Ckip-1* 3′ untranslated region exhibits distinct expression and location from that of *Ckip-1* coding sequence region. It activates CaMKK2-AMPK-PPARα-CPT1b axis by sponging Let-7f. Ultimately, 3′ untranslated region inhibits cardiac hypertrophy with a CKIP-1 protein-independent mechanism through reversed lipotoxicity and increased ATP supply. Data are mean ± SD. Statistical analysis for the comparison of two groups was performed using two-tailed unpaired Student's *t*-test. Statistical differences among groups were analysed by two-way ANOVA with Šídák *post hoc* test to determine group differences. Each statistical comparison undertaken has an assigned *P*-value (adjusted for multiplicity). Differences were considered significant at *P*-value <0.05. H&E, haematoxylin and eosin; TAC, transverse aortic constriction; TG, transgenic; UTR, untranslated region; WGA, wheat germ agglutinin.

DJ; ESC Scientific Document Group. 2015 ESC Guidelines for the management of patients with ventricular arrhythmias and the prevention of sudden cardiac death: the Task Force for the management of patients with ventricular arrhythmias and the prevention of sudden cardiac death of the European Society of Cardiology (ESC). Endorsed by: Association for European Paediatric and Congenital Cardiology (AEPC). *Eur Heart J* 2015;**36**:2793–2867.
5. Stanley WC, Recchia FA, Lopaschuk GD. Myocardial substrate metabolism in the normal and failing heart. *Physiol Rev* 2005;**85**:1093–1129.
6. Jacoby D, McKenna WJ. Genetics of inherited cardiomyopathy. *Eur Heart J* 2012;**33**:296–304.
7. Heusch G, Libby P, Gersh B, Yellon D, Böhm M, Lopaschuk G, Opie L. Cardiovascular remodelling in coronary artery disease and heart failure. *Lancet* 2014;**383**:1933–1943.
8. Elliott PM, Anastasakis A, Borger MA, Borggrefe M, Cecchi F, Charron P, Hagege AA, Lafont A, Limongelli G, Mahrholdt H, McKenna WJ, Mogensen J, Nihoyannopoulos P, Nistri S, Pieper PG, Pieske B, Rapezzi C, Rutten FH, Tillmanns C, Watkins H. 2014 ESC Guidelines on diagnosis and management of hypertrophic cardiomyopathy: the Task Force for the diagnosis and management of hypertrophic cardiomyopathy of the European Society of Cardiology (ESC). *Eur Heart J* 2014;**35**:2733–2779.
9. van den Hoogenhof MM, Pinto YM, Creemers EE. RNA splicing: regulation and dysregulation in the heart. *Circ Res* 2016;**118**:454–468.
10. Gomes CPC, Schroen B, Kuster GM, Robinson EL, Ford K, Squire IB, Heymans S, Martelli F, Emanueli C, Devaux Y; EU-CardioRNA COST Action (CA17129). Regulatory RNAs in heart failure. *Circulation* 2020;**141**:313–328.
11. Gao C, Wang Y. mRNA metabolism in cardiac development and disease: life after transcription. *Physiol Rev* 2020;**100**:673–694.
12. Keene JD. RNA regulons: coordination of post-transcriptional events. *Nat Rev Genet* 2007;**8**:533–543.
13. Herzel L, Ottoz DSM, Alpert T, Neugebauer KM. Splicing and transcription touch base: co-transcriptional spliceosome assembly and function. *Nat Rev Mol Cell Biol* 2017;**18**:637–650.
14. Mignone F, Gissi C, Liuni S, Pesole G. Untranslated regions of mRNAs. *Genome Biol* 2002;**3**:REVIEWS0004.
15. Chatterjee S, Pal JK. Role of 5'- and 3'-untranslated regions of mRNAs in human diseases. *Biol Cell* 2009;**101**:251–262.
16. Srivastava AK, Lu Y, Zinta G, Lang Z, Zhu JK. UTR-dependent control of gene expression in plants. *Trends Plant Sci* 2018;**23**:248–259.
17. Kuersten S, Goodwin EB. The power of the 3' UTR: translational control and development. *Nat Rev Genet* 2003;**4**:626–637.
18. Mayr C. What are 3' UTRs doing? *Cold Spring Harb Perspect Biol* 2019;**11**:a034728.
19. Conne B, Stutz A, Vassalli JD. The 3' untranslated region of messenger RNA: a molecular 'hotspot' for pathology? *Nat Med* 2000;**6**:637–641.
20. Mahadevan MS, Yadava RS, Yu Q, Balijepalli S, Frenzel-McCardell CD, Bourne TD, Phillips LH. Reversible model of RNA toxicity and cardiac conduction defects in myotonic dystrophy. *Nat Genet* 2006;**38**:1066–1070.
21. Mercer TR, Wilhelm D, Dinger ME, Soldà G, Korbie DJ, Glazov EA, Truong V, Schwenke M, Simons C, Matthaei KI, Saint R, Koopman P, Mattick JS. Expression of distinct RNAs from 3' untranslated regions. *Nucleic Acids Res* 2011;**39**:2393–2403.
22. Malka Y, Steiman-Shimony A, Rosenthal E, Argaman L, Cohen-Daniel L, Arbib E, Margalit H, Kaplan T, Berger M. Post-transcriptional 3'-UTR cleavage of mRNA transcripts generates thousands of stable uncapped autonomous RNA fragments. *Nat Commun* 2017;**8**:2029.
23. Kocabas A, Duarte T, Kumar S, Hynes MA. Widespread differential expression of coding region and 3' UTR sequences in neurons and other tissues. *Neuron* 2015;**88**:1149–1156.
24. Jenny A, Hachet O, Závorszky P, Cyrklaff A, Weston MD, Johnston DS, Erdélyi M, Ephrussi A. A translation-independent role of oskar RNA in early Drosophila oogenesis. *Development* 2006;**133**:2827–2833.
25. Ritterhoff J, Tian R. Metabolism in cardiomyopathy: every substrate matters. *Cardiovasc Res* 2017;**113**:411–421.
26. Neubauer S. The failing heart—an engine out of fuel. *N Engl J Med* 2007;**356**:1140–1151.
27. Lopaschuk GD, Ussher JR, Folmes CD, Jaswal JS, Stanley WC. Myocardial fatty acid metabolism in health and disease. *Physiol Rev* 2010;**90**:207–258.
28. Goldberg IJ, Trent CM, Schulze PC. Lipid metabolism and toxicity in the heart. *Cell Metab* 2012;**15**:805–812.
29. Kienesberger PC, Pulinilkunnil T, Nagendran J, Dyck JR. Myocardial triacylglycerol metabolism. *J Mol Cell Cardiol* 2013;**55**:101–110.
30. Sharma S, Adrogue JV, Golfman L, Uray I, Lemm J, Youker K, Noon GP, Frazier OH, Taegtmeyer H. Intramyocardial lipid accumulation in the failing human heart resembles the lipotoxic rat heart. *FASEB J* 2004;**18**:1692–1700.
31. D'Souza K, Nzirorera C, Kienesberger PC. Lipid metabolism and signaling in cardiac lipotoxicity. *Biochim Biophys Acta* 2016;**1861**:1513–1524.
32. Zaha VG, Young LH. AMP-activated protein kinase regulation and biological actions in the heart. *Circ Res* 2012;**111**:800–814.
33. Zhang P, Hu X, Xu X, Fassett J, Zhu G, Viollet B, Xu W, Wiczer B, Bernlohr DA, Bache RJ, Chen Y. AMP activated protein kinase-alpha2 deficiency exacerbates pressure-overload-induced left ventricular hypertrophy and dysfunction in mice. *Hypertension* 2008;**52**:918–924.
34. Zhang C, Seo J, Murakami K, Salem ESB, Bernhard E, Borra VJ, Choi K, Yuan CL, Chan CC, Chen X, Huang T, Weirauch MT, Divanovic S, Qi NR, Thomas HE, Mercer CA, Siomi H, Nakamura T. Hepatic Ago2-mediated RNA silencing controls energy metabolism linked to AMPK activation and obesity-associated pathophysiology. *Nat Commun* 2018;**9**:3658.
35. Ling S, Sun Q, Li Y, Zhang L, Zhang P, Wang X, Tian C, Li Q, Song J, Liu H, Kan G, Cao H, Huang Z, Nie J, Bai Y, Chen S, Li Y, He F, Zhang L, Li Y. CKIP-1 inhibits cardiac hypertrophy by regulating class II histone deacetylase phosphorylation through recruiting PP2A. *Circulation* 2012;**126**:3028–3040.
36. Yang KC, Yamada KA, Patel AY, Topkara VK, George I, Cheema FH, Ewald GA, Mann DL, Nerbonne JM. Deep RNA sequencing reveals dynamic regulation of myocardial noncoding RNAs in failing human heart and remodeling with mechanical circulatory support. *Circulation* 2014;**129**:1009–1021.
37. Mihaylova MM, Shaw RJ. The AMPK signalling pathway coordinates cell growth, autophagy and metabolism. *Nat Cell Biol* 2011;**13**:1016–1023.
38. Mayr C. Regulation by 3'-untranslated regions. *Annu Rev Genet* 2017;**51**:171–194.
39. Steri M, Idda ML, Whalen MB, Orrù V. Genetic variants in mRNA untranslated regions. *Wiley Interdiscip Rev RNA* 2018;**9**:e1474.
40. Orengo JP, Chambon P, Metzger D, Mosier DR, Snipes GJ, Cooper TA. Expanded CTG repeats within the DMPK 3' UTR causes severe skeletal muscle wasting in an inducible mouse model for myotonic dystrophy. *Proc Natl Acad Sci USA* 2008;**105**:2646–2651.
41. Mayr C, Bartel DP. Widespread shortening of 3'UTRs by alternative cleavage and polyadenylation activates oncogenes in cancer cells. *Cell* 2009;**138**:673–684.
42. Bai Y, Zhou K, Doudna JA. Hepatitis C virus 3'UTR regulates viral translation through direct interactions with the host translation machinery. *Nucleic Acids Res* 2013;**41**:7861–7874.
43. Creemers EE, Bawazeer A, Ugalde AP, van Deutekom HW, van der Made I, de Groot NE, Adriaens ME, Cook SA, Bezzina CR, Hubner N, van der Velden J, Elkon R, Agami R, Pinto YM. Genome-wide polyadenylation maps reveal dynamic mRNA 3'-end formation in the failing human heart. *Circ Res* 2016;**118**:433–438.
44. Ma W, Mayr C. A membraneless organelle associated with the endoplasmic reticulum enables 3'UTR-mediated protein-protein interactions. *Cell* 2018;**175**:1492–1506.e19.
45. Elkon R, Ugalde AP, Agami R. Alternative cleavage and polyadenylation: extent, regulation and function. *Nat Rev Genet* 2013;**14**:496–506.
46. Mohan N, Kumar V, Kandala DT, Kartha CC, Laishram RS. A splicing-independent function of RBM10 controls specific 3' UTR processing to regulate cardiac hypertrophy. *Cell Rep* 2018;**24**:3539–3553.
47. Liu X, Beaudoin JD, Davison CA, Kosmaczewski SG, Meyer BI, Giraldez AJ, Hammarlund M. A functional non-coding RNA is produced from xbp-1 mRNA. *Neuron* 2020;**107**:854–863.e6.
48. Li W, Ma M, Feng Y, Li H, Wang Y, Ma Y, Li M, An F, Guo H. EIN2-directed translational regulation of ethylene signaling in Arabidopsis. *Cell* 2015;**163**:670–683.
49. Qi D, Atsina K, Qu L, Hu X, Wu X, Xu B, Piecychna M, Leng L, Fingerle-Rowson G, Zhang J, Bucala R, Young LH. The vestigial enzyme D-dopachrome tautomerase protects the heart against ischemic injury. *J Clin Invest* 2014;**124**:3540–3550.
50. Vega RB, Kelly DP. Cardiac nuclear receptors: architects of mitochondrial structure and function. *J Clin Invest* 2017;**127**:1155–1164.
51. Meng R, Pei Z, Zhang A, Zhou Y, Cai X, Chen B, Liu G, Mai W, Wei J, Dong Y. AMPK activation enhances PPARα activity to inhibit cardiac hypertrophy via ERK1/2 MAPK signaling pathway. *Arch Biochem Biophys* 2011;**511**:1–7.
52. Brown NF, Weis BC, Husti JE, Foster DW, McGarry JD. Mitochondrial carnitine palmitoyltransferase I isoform switching in the developing rat heart. *J Biol Chem* 1995;**270**:8952–8957.
53. Fu L, Zhang L. Physiological functions of CKIP-1: from molecular mechanisms to therapy implications. *Ageing Res Rev* 2019;**53**:100908.
54. Ling S, Li Y, Zhong G, Zheng Y, Xu Q, Zhao D, Sun W, Jin X, Li H, Li J, Sun H, Cao D, Song J, Liu C, Yuan X, Wu X, Zhao Y, Liu Z, Li Q, Li Y. Myocardial CKIP-1 overexpression protects from simulated microgravity-induced cardiac remodeling. *Front Physiol* 2018;**9**:40.